Light–Switchable and Monodisperse Conjugated Polymer Particles

4 AUTHORS, INCLUDING:

Naveed Anwar
RWTH Aachen University
3 PUBLICATIONS **16** CITATIONS

SEE PROFILE

Alexander Kuehne
DWI - Leibniz Institute for Interactive Materials
35 PUBLICATIONS **214** CITATIONS

SEE PROFILE

Light-Switchable and Monodisperse Conjugated Polymer Particles

Naveed Anwar, Thomas Willms, Benjamin Grimme, and Alexander J. C. Kuehne*

Interactive Materials Research, DWI at RWTH Aachen University, 52056 Aachen, Germany

S *Supporting Information*

ABSTRACT: We present a novel class of light-responsive particles for fluorescence modulation at low switching doses. The particles also exhibit phase-changing and shape-shifting behavior. The monodisperse conjugated polymer particles with incorporated light-switchable azobenzene moieties are prepared in a Suzuki-Miyaura dispersion polymerization. The influence of the molecular structure and the *trans*-to-*cis* switching behavior on the photonic performance are investigated. The polymer particles present ideal candidates for responsive organic photonics and as high resolution marker systems for biomedical applications.
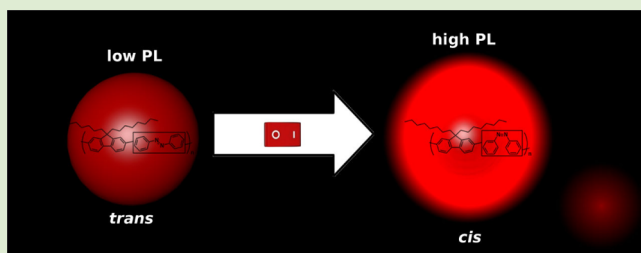
Light-responsive moieties are a powerful tool to switch the physical properties of a material system. Azobenzenes are a well-established class of light-responsive units, and their switching mechanism is well understood.[1] Upon excitation with ultraviolet (UV) light, a conformational *trans*-to-*cis* transition occurs and the molecular as well as the electronic structure change. The azobenzene moiety reverts back to the *trans*-conformation thermally or by exposing the system to radiation of the green to yellow spectrum. Azobenzenes have been employed in light-responsive films,[2] encapsulants,[3] and surfactants.[4] In the latter, the *trans*-to-*cis* switch evokes a change in the entire molecular structure. As such, the switchable surface active agent can no longer minimize the interfacial energy effectively and emulsions and encapsulants can be broken to release the stabilized or encapsulated cargo. Further applications of switchable materials lie in the fields of biological markers[5] and photonic systems,[6] where the *trans*-to-*cis* switch induces changes in the refractive index and absorption. This change gives rise to fluorescence enhancement or quenching by Förster Resonant Energy Transfer (FRET).[5,7] Switching of azobenzene units within π-conjugated polymers has been studied extensively in solution, and depending on how the switchable unit is interacting with the conjugated polymer backbone, the absorption and fluorescence performance can be modulated.[5,7−10] The *trans*-to-*cis* switch can either improve or quench fluorescence depending on the electronic donor/acceptor character of the comonomers and their bandgaps. Recently, switchable moieties have been incorporated into conjugated polymer particles for highly sensitive bioimaging techniques. The switchable particles have been applied to specifically stain membrane proteins in cells.[5] By UV irradiation, the fluorescence signal of the polymer particles can be modulated allowing improved performance in super-resolution microscopy. However, these conjugated polymer particles have been prepared by emulsion processes leading to polydisperse samples. Consequently, photonic effects, which

arise from monodisperse particle samples through their self-assembly into periodic structures cannot be exploited.[11] Also, polydisperse particles are less specific when applied as markers and probes in biological systems. Processes like endocytosis and diffusion are size-dependent; thus, a large fraction of a polydisperse set of particles will not enter and stain cells effectively.[12] Recently, we reported a dispersion polymerization, which allows the preparation of monodisperse conjugated polymer particles.[13] Monodisperse conjugated polymer particles with the additional functionality of a switchable moieties will enable the preparation of responsive and bistable organic photonics. Self-assemblies of such monodisperse particles would act as switchable photonic crystals. Fluorescence modulation will allow high sensitivity when these particles are applied as biological marker systems. Furthermore, conjugated polymer particles show less bleaching than single molecule labels, they are not cytotoxic, and they do not show blinking as many inorganic quantum dot probes.[14−16] As such, switchable conjugated polymer particles would constitute ideal candidates for a novel class of fluorescent biological markers.

Here we report the synthesis of three types of switchable and monodisperse conjugated polymer particles. Suzuki-Miyaura dispersion polymerization is applied to produce particles of alternating fluorene-*alt*-azobenzene polymers. The size of the particles can be easily adjusted and *trans*-to-*cis* switching results in fluorescence intensification.

To obtain three different types of switchable conjugated polymer particles we employ the diboronic acid ester of fluorene together with dibromo azobenzene derivatives using a palladium catalyst, potassium *t*-butoxide as base and 1-propanol as solvent, as shown in Scheme 1. Upon reaching of a critical molecular weight, the conjugated polymers precipitate into

Scheme 1. Suzuki-Miyaura Dispersion Polymerization of Three Types of Switchable Colloids: Incorporation of the Azobenzene Unit along the Polymer Backbone (P1), Perpendicular to the Polymer Chain (P2), and Electronically Decoupled from the Polymer Backbone by Means of an Alkyl-Spacer (P3)
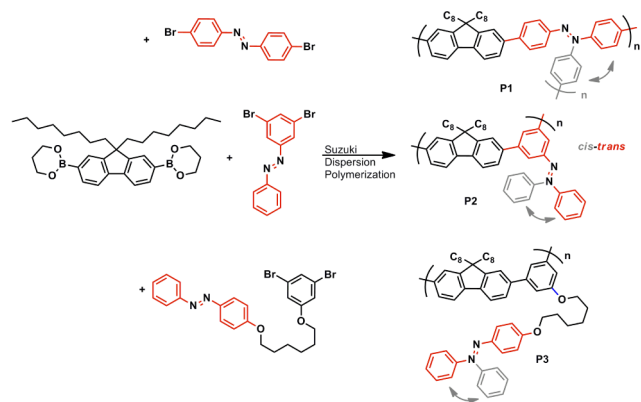
nuclei, which are stabilized by Triton X-45 and poly-(vinylpyrrolidone-*co*-vinyl acetate) (PVPVA).[13] Subsequently, further polymers precipitate and condense onto the nuclei, which all grow at the same rate to produce monodisperse particles.[17] To determine the critical molecular weight, upon which the polymers precipitate to form particles during the dispersion polymerization, a representative sample of each type of particle is dissolved in chloroform and analyzed by gel permeation chromatography (see Table 1). For all three types

Table 1. Properties of the Switchable Conjugated Polymer Particles

entry	M_w (Da)	PDI	λ^E_{max} [trans] (nm)	λ^I_{max} [cis] (nm)	D_{PSS} (nJ/cm^2)
P1	13423	2.26	444	612	41
P2	13088	1.14	421	545	22
P3	49622	2.65	397	528	32

of particles we obtain moderately high molecular weights of up to about 50 kDa. The molecular weight of **P1** and **P2** is limited to about 13 kDa. **P3** has more flexible side groups and, thus, it is more soluble, and much higher molecular weights can be obtained before the polymer chains precipitate into nuclei. The polymerization follows a polycondensation mechanism; however, a PDI of below 2 is not surprising, considering that the molecular weight distribution will have a sharp cutoff toward higher values due to the precipitation of the polymer chains at the critical molecular weight for solubility. The higher PDI values of **P1** and **P3** as compared to **P2** could be an effect of variations in solubility, the azobenzene monomer purity, or residual PVPVA stabilizer polymer during GPC analysis. The PDIs are similar to those observed previously in Suzuki-Miyaura dispersion polymerizations.[13]

We apply 4,4′-dibromoazobenzene to obtain conjugated polymer particles with the azobenzene unit oriented along the polymer backbone (**P1**). This synthesis produces particles, where the entire polymer chain is subject to extensive and space-demanding motion upon *trans*-to-*cis* switching (see Scheme 1). By contrast, 3,5-dibromoazobenzene as a comonomer leads to particles with the azobenzene unit perpendicular to the polymer backbone. The azobenzene unit

is in conjugation with the conjugated polymer backbone but *trans*-to-*cis* switching results in the motion of merely the peripheral phenyl ring and not the entire backbone (**P2**). The third switchable comonomer is produced by coupling a 4-hydroxyazobenzene to 3,5-dibromophenol using a hexyl spacer. The polymerization with diboronic acid ester fluorene yields particles with switchable units that are decoupled from the π-conjugated polymer backbone (**P3**). The monomers are synthesized in accordance with established literature procedures.[18,19] The resulting particles of **P1** are obtained as thin platelets with square faces, whereas particles of **P2** and **P3** are obtained as monodisperse and perfectly round particles (see Figure 1a−c). The anisometric shape of the **P1** particles is
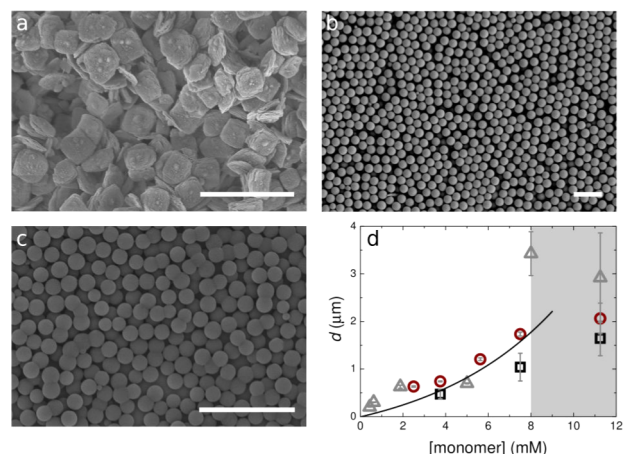

Figure 1. SEM images of (a) narrowly dispersed platelets composed of **P1**, (b) monodisperse **P2**, and (c) **P3** particles. The scale bar represents 2 μm. (d) The particle size can be tuned by varying the monomer concentration: **P1** (black squares), **P2** (red circles), and **P3** (gray triangles). The black line is a guide to the eye.

surprising but can be explained by a preferential direction of growth during the dispersion polymerization. A recent report on the synthesis of the **P1** polymer, describes a helical molecular structure of the polymer in the *trans*-conformation. In solution this helical structure leads to crystallization into aggregates.[9] Upon *trans*-to-*cis* switching the aggregates redissolve. Here, the anisometric growth of the particles during dispersion polymerization will be a result of the reported structure as helices aggregate faster side-by-side than end-to-end, leading to the platelet shape. To verify this hypothesis, we perform X-ray powder diffraction (XRD) analysis on dried samples of the polymer particles. The **P1** particles show distinct XRD peaks in compliance with columnar packing (see Figure S1). By contrast, **P2** and **P3** exhibit only broad XRD features, which represent an amorphous polymer morphology consistent with the spherical shape of the particles. To access a wide range of applications, tunability in particle size is imperative. We control the size of the particle via the monomer concentration during synthesis. The size of the narrowly dispersed platelets and monodisperse spherical particles is determined by electron microscopy image analysis, as well as by dynamic light scattering, as indicated by the error bars in Figure 1d. The particle size can be adjusted from about 200 nm to above 1.5 μm. The **P2** and **P3** particles remain monodisperse with a polydispersity of less than 4% below a concentration of about 8 mM, as indicated by the shaded area in Figure 1d. This concentration can be considered the critical threshold, above

which the particles become polydisperse. Here, secondary nucleation occurs during synthesis, limiting monodispersity (see Figure 1d).

To investigate the *trans*-to-*cis* switching characteristics of the polymer particles, UV/vis extinction, and fluorescence experiments are conducted. Structurally, the azobenzene group is moved away from being a part of the polymer backbone in **P1** to the periphery in **P2** to being electronically decoupled from the backbone in **P3**. This displacement also shows in the spectral properties of the polymer particles. The extinction and fluorescence maxima shift from longer wavelengths to higher energies from **P1** to **P3**. This is the effect of changing the electronic push−pull system along the polymer chain for **P1** to a backbone-azobenzene FRET pair in the case of **P3**. To demonstrate the switching behavior of all three types of particles, dispersions are exposed to a broadband UV source with an emission maximum at 380 nm and the change in extinction is monitored over time. Furthermore, the fluorescence of individual particles is recorded as a function of the radiation dose at 405 nm using confocal microscopy (see Figures 2 and S2). Upon UV-irradiation, the extinction of the
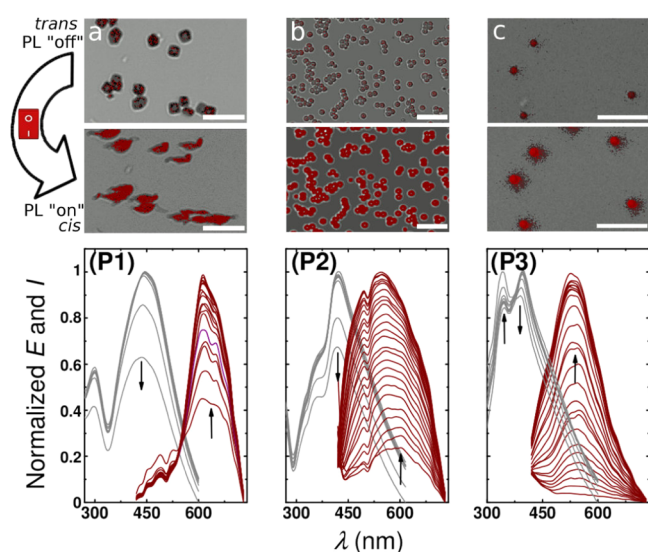

Figure 2. Switching of the azobenzene conjugated polymer particles. Confocal microscopy images of (a) **P1**, (b) **P2**, and (c) **P3** particles before (above) and after UV irradiation (middle) and the absorption and fluorescence spectra of the particles (below). The scale bar represents 5 μm.

dispersed particles decreases due to the *trans*-to-*cis* switching. An increase in absorption at lower energies due to $n \rightarrow \pi^*$ of the *cis*-conformation is not visible here. This band is usually very weak and will be concealed by the extinction peaks, which broadened due to scattering of the particles. However, for **P3** a concomitant increase in extinction is visible at higher energies (342 nm). Due to the electronic decoupling of the conjugated backbone and the azobenzene moiety the characteristic $\pi \rightarrow \pi^*$ transition of the *cis*-conformation is visible.[1] For all three types of particles, an increase in fluorescence is observed with *trans*-to-*cis* switching. This can also be observed in confocal microscopy, where the particles show improved fluorescence after irradiation at 405 nm (see Figure 2a−c). Simplified, this behavior is attributed to fluorescence quenching between the fluorene donor and the *trans*-azobenzene acceptor units. In the *trans*-conformation fluorescence quenching can occur due to

the conical intersection in the S_0/S_1 energy landscape of the azobenzene isomers.[20] Nonradiative decay via the conical intersection is more probably for azobenzene in the *trans*-conformation.[21] However, when the azobenzene units are switched into the *cis*-conformation, their electronic bandgap is slightly increased and the overlap integrals between fluorescence of the fluorene donor and the absorption of the azobenzene acceptor will be larger. This increased overlap integral allows a more efficient energy transfer into the *cis*-azobenzene unit, which fluoresces in the visible spectrum with less chance to decay nonradiatively.[21] This explanation treats the fluorene and azobenzene units as separate entities; however, in the real polymer particle there will be extended π-conjugation and interchain effects, which influence the quenching and energy transfer processes. Further studies will have to be performed to fully understand the underlying molecular orbital structures and the corresponding quenching and intensification mechanism in detail.

Due to the molecular structure of the polymers inside the particles, switching is much slower for **P1** than for **P2** and **P3** (see Figure S2 and Table 1). This can be explained by the fact that the entire backbone of a polymer molecule and the neighboring polymer chains need to move in concert for the diazobenzene monomer units to switch. During switching the crystalline platelets change shape, as can be seen in the confocal microscopy images in Figure 2a. This is clearly an effect of the molecular rearrangement of the crystallized polymer chains, while the azobenzene units isomerize to the *cis*-form. **P2** and **P3** both reach their photostationary state at lower irradiation doses (D_{PSS}) without losing their spherical shape (see Figure 2 and Table 1). For these types of particles, the azobenzene unit can switch from *trans* to *cis* without affecting the geometry of the polymer backbone. When the particle samples are irradiated with green light of 561 nm, the azobenzene *cis*-form changes back to *trans*. This isomeric switching can be observed as a sharp drop in fluorescence at low doses for **P2** and **P3** (see Figure S2). By contrast, the drop in fluorescence intensity for **P1** decreases more slowly. Furthermore, the **P1** particles do not regain their platelet shape, but remain deformed, and *cis*-to-*trans* switching is not fully reversible (see Figures 2 and S2). The change from crystalline to an amorphous morphology is associated with the glass transition, which is usually traversed by heating the material. Here, the transition is induced by exposure to light, which provides an intriguing system to study phase-change materials.

The method for synthesizing such switchable conjugated polymer particles is highly versatile and other types of switchable monomers could also be applied, provided they are dihalogenated to participate in the palladium-catalyzed coupling reaction. With their fast switching characteristics, amorphous morphology, and precise monodispersity, **P2** and **P3** particles present ideal candidates for self-assembled switchable photonics. The particles can be assembled into coatings,[22] where they create switchable physical color by diffraction or in photonic crystals for wavelength conversion[23] with a switchable band gap or as colloidal laser resonators.[5,24] **P1** particles display a change in shape for switching from the *trans* to the *cis*-conformation together with an increase in fluorescence intensity. This will enable applications as shape-shifting or phase-change materials. All three types of particles could be applied as switchable probes and markers for super-resolution imaging in the biomedical field.[16,25]

■ ASSOCIATED CONTENT

ⓈSupporting Information

Synthesis and characterization of the synthesized particles, including XRD (Figure S1) and dose related *trans*-to-*cis* switching behavior (Figure S2). This material is available free of charge via the Internet at http://pubs.acs.org.

■ AUTHOR INFORMATION

Corresponding Author

*E-mail: kuehne@dwi.rwth-aachen.de.

Notes

The authors declare no competing financial interest.

■ ACKNOWLEDGMENTS

■ REFERENCES

(1) Bandara, H. M. D.; Burdette, S. C. *Chem. Soc. Rev.* **2012**, *41*, 1809−1825.

(2) Yu, Y.; Maeda, T.; Mamiya, J.-I.; Ikeda, T. *Angew. Chem., Int. Ed.* **2007**, *46*, 881−883.

(3) Li, L.; Rosenthal, M.; Zhang, H.; Hernandez, J. J.; Drechsler, M.; Phan, K. H.; Rütten, S.; Zhu, X.; Ivanov, D. a.; Möller, M. *Angew. Chem., Int. Ed.* **2012**, *51*, 11616−11619.

(4) Khoukh, S.; Perrin, P.; Bes de Berc, F.; Tribet, C. *ChemPhysChem* **2005**, *6*, 2009−2012.

(5) Chan, Y.-H.; Gallina, M. E.; Zhang, X.; Wu, I.-C.; Jin, Y.; Sun, W.; Chiu, D. T. *Anal. Chem.* **2012**, *84*, 9431−9438.

(6) Russew, M.-M.; Hecht, S. *Adv. Mater.* **2010**, *22*, 3348−3360.

(7) Harbron, E. J.; Vicente, D. a.; Hoyt, M. T. *J. Phys. Chem. B* **2004**, *108*, 18789−18792.

(8) Izumi, A.; Nomura, R.; Masuda, T. *Macromolecules* **2001**, *34*, 4342−4347.

(9) Zhang, W.; Yoshida, K.; Fujiki, M.; Zhu, X. *Macromolecules* **2011**, *44*, 5105−5111.

(10) Li, Z.; Zeng, Q.; Yu, G.; Li, Z.; Ye, C.; Liu, Y.; Qin, J. *Macromol. Rapid Commun.* **2008**, *29*, 136−141.

(11) Kuehne, A. J. C.; Weitz, D. A. *Chem. Commun.* **2011**, *47*, 12379−12381.

(12) Zhang, S.; Li, J.; Lykotrafitis, G.; Bao, G.; Suresh, S. *Adv. Mater.* **2009**, *21*, 419−424.

(13) Kuehne, A. J. C.; Gather, M. C.; Sprakel, J. *Nat. Commun.* **2012**, *3*, 1088.

(14) Wu, C.; Bull, B.; Szymanski, C.; Christensen, K.; McNeill, J. *ACS Nano* **2008**, *2*, 2415−2423.

(15) Kim, S.; Lim, C.-K.; Na, J.; Lee, Y.-D.; Kim, K.; Choi, K.; Leary, J. F.; Kwon, I. C. *Chem. Commun.* **2010**, *46*, 1617−1919.

(16) Rahim, N. A. A.; McDaniel, W.; Bardon, K.; Srinivasan, S.; Vickerman, V.; So, P. T. C.; Moon, J. H. *Adv. Mater.* **2009**, *21*, 3492−3496.

(17) Kawaguchi, S.; Ito, K. *Adv. Polym. Sci.* **2005**, *175*, 299−328.

(18) Burns, J.; McCombie, H.; Scarborough, H. *J. Chem. Soc.* **1928**, 2928−2936.

(19) Liu, J.; Li, L.; Pei, Q. *Macromolecules* **2011**, *44*, 2451−2456.

(20) Tiberio, G.; Muccioli, L.; Berardi, R.; Zannoni, C. *ChemPhysChem* **2010**, *11*, 1018−28.

(21) Satzger, H.; Spörlein, S.; Root, C.; Wachtveitl, J.; Zinth, W.; Gilch, P. *Chem. Phys. Lett.* **2003**, *372*, 216−223.

(22) Finlayson, C. E.; Spahn, P.; Snoswell, D. R. E.; Yates, G.; Kontogeorgos, A.; Haines, A. I.; Hellmann, G. P.; Baumberg, J. J. *Adv. Mater.* **2011**, *23*, 1540−1544.

(23) Deutsch, M.; Vlasov, Y. a.; Norris, D. J. *Adv. Mater.* **2000**, *12*, 1176−1180.

(24) Shkunov, M.; Vardeny, Z.; DeLong, M.; Polson, R.; Zakhidov, A. A.; Baughman, R. *Adv. Funct. Mater.* **2002**, *12*, 21−26.

(25) Yoo, J.-W.; Mitragotri, S. *Proc. Natl. Acad. Sci. U.S.A.* **2010**, *107*, 11205−10.